SPIE Proceedings BIOS 2010, Ophthalmic Technologies XX, Vol. 7550

Improved safety of retinal photocoagulation with a shaped beam and modulated pulse

Christopher Sramek[*1], Jefferson Brown[1], Yannis M. Paulus[2], Hiroyuki Nomoto[2], Daniel Palanker[1, 2]

[1]Hansen Experimental Physics Laboratory, [2]Department of Ophthalmology
Stanford University, Stanford, CA

ABSTRACT

Shorter pulse durations help confine thermal damage during retinal photocoagulation, decrease treatment time and minimize pain. However, safe therapeutic window (the ratio of threshold powers for rupture and mild coagulation) decreases with shorter exposures. A ring-shaped beam enables safer photocoagulation than conventional beams by reducing the maximum temperature in the center of the spot. Similarly, a temporal pulse modulation decreasing its power over time improves safety by maintaining constant temperature for a significant portion of the pulse. Optimization of the beam and pulse shapes was performed using a computational model. *In vivo* experiments were performed to verify the predicted improvement. With each of these approaches, the pulse duration can be decreased by a factor of two, from 20 ms down to 10 ms while maintaining the same therapeutic window.

Keywords: retinal photocoagulation, damage threshold, retinal thermal damage

1. INTRODUCTION

Laser photocoagulation, the standard of care for several retinopathies[1-4], involves the application of pulses of 100 – 500 ms in duration, often resulting in collateral thermal damage to the inner retina[5]. In patterned scanning laser photocoagulation, patterns of 4 to 50 exposures are delivered sequentially within the eye fixation time, with pulse durations in the range of 20 ms[6]. These shorter exposures have been shown to be less painful and as efficacious as traditional retinal photocoagulation[5,7], while targeting the retinal pigment epithelium (RPE) and outer retina more selectively[8]. However, coagulation at shorter pulse durations requires higher peak temperatures, increasing the potential for photomechanical injury due to vaporization and subsequent rupture of Bruch's membrane[9]. This leads to narrowing of the safe therapeutic window (TW), defined as the ratio of power for producing a rupture to that of mild coagulation, which approaches unity at 1 ms[10].

It is thus desirable to increase the therapeutic window in order to allow for shorter duration pulses to be used in photocoagulation. One approach to this end is to modify the shape of the treatment beam. With conventional flat-top or Gaussian radial beam profiles, heat diffusion during the pulse results in an elevated temperature at the beam center. Such over-heating results in a higher maximum temperature than necessary to produce the desired retinal coagulation, and increases the probability of rupture. A beam shape with a lower intensity in the center compensates for the effects of thermal diffusion, resulting in a more uniform temperature profile and thermal damage zone. This absence of central overheating is expected to result in a wider therapeutic window.

A second approach to increasing the safe therapeutic window is to modify the temporal structure of the pulse. Conventional pulses of constant power (square pulse shape) result in an increasing temperature during the pulse, asymptotically approaching a steady-state value for long exposures. Thermal cellular damage in the millisecond regime is often described using the Arrhenius model[11,12]. It assumes a decrease in concentration of viable cells $D(\tau)/D_0$ as an exponential integral of the temperature time-course:

[*] csramek@stanford.edu; phone 1 650 723-0130; http://www.stanford.edu/~palanker/lab/

$$\Omega = A\int_0^{\tau} \exp\left(-\frac{E^*}{R\cdot T(t)}\right)dt = -\ln\left(\frac{D(\tau)}{D_0}\right) \quad (1)$$

where E* is the activation energy, A is the rate constant, and R is the gas constant. The increasing temperature with time produced by a square laser pulse leads to an exponential increase in the reaction rate at the end of the pulse, while most of the pulse duration does not effectively contribute to the tissue coagulation.

The entire pulse length can be more efficiently utilized by varying the laser power to compensate for heat diffusion. Such a pulse consists of an initial constant-power phase to bring the temperature up to a desired level and a slow decrease to maintain this temperature. With such a pulse shape, a larger fraction of the pulse duration effectively contributes to the Arrhenius integral, which allows for a shorter pulse length to be used for coagulation at a given peak temperature.

Precise estimation of the optimal beam and pulse shapes requires the solution of the heat conduction equation, which can account for differences in heat deposition in various retinal layers, inhomogeneities due to pigmentation variation, and convective cooling due to blood perfusion. Due to these factors, computational modeling can greatly assist in calculating optimal beam and pulse parameters.

We report the results of semi-analytical and finite-element modeling in conjunction with *in vivo* experimental verification of improvements in safety of retinal photocoagulation with both a ring-shaped beam and pulses with temporal power modulation.

2. MATERIALS AND METHODS

2.1 Semi-analytical model

To estimate optimal temporal pulse shapes, a simple semi-analytical model of retinal light absorption and heat conduction was constructed. This model approximated the posterior pole as three homogeneous layers, a 4 μm retinal pigment epithelium between 100 μm neurosensory retinal and 70 μm choroidal layers. An axi-symmetric heat conduction model was coupled with an Arrhenius damage model. The Green's function solution to the heat conduction equation[13] was numerically integrated in MATLAB (v 7.4, MathWorks, Natick, MA) for the temperature rise at the top of the RPE in the beam center at the end of a pulse duration τ:

$$\Delta T(\tau) = \frac{k\cdot P}{2(\pi k)^{3/2}\cdot \rho c_p R^2}\int_0^{\tau} dt' \frac{f(t'-\tau)}{\sqrt{t'}}\left(1-e^{-\frac{R^2}{4kt'}}\right)Z_{\text{int}}(t') \quad (2)$$

where f(t) is the pulse shape normalized to unity, P is the laser power, R is the beam radius (assumed to be 60 μm, flat-top radial distribution), ρc_p is the density and heat capacity of water and Z_{int} is an integral corresponding to energy deposition in the RPE and choroidal layers by the absorbed laser beam:

$$Z_{\text{int}}(t') = \alpha_1\int_0^{z_{RPE}} dz' e^{-\frac{z'^2}{4kt'}-\alpha_1 z'} + \alpha_2\int_{z_{RPE}}^{z_{CH}} dz' e^{-\frac{z'^2}{4kt'}-\alpha_2 z'} \quad (3)$$

The absorption coefficients for the RPE and choroid (α_1 and α_2 respectively) and RPE thickness z_{RPE} were taken from a more extensive finite-element retinal photocoagulation model described elsewhere[14].

The pulse shape included two distinct phases: a constant power phase ($t < \tau_1$) and a decreasing power phase ($\tau_1 < t < \tau$). Vectors $\mathbf{f}(\tau_1, \tau)$ representing the pulse shape f(t) were constructed for pulse durations τ of 5, 10 and 20 ms and τ_1 between $0.01\cdot\tau$ and $0.99\cdot\tau$. The decreasing power phase was approximated as a spline defined at 20 evenly spaced points. A multi-parameter numerical optimization was performed for spline points that minimized the mean-square error of computed ΔT(t) and constant temperature on the interval $[\tau_1,\tau]$ for all (τ_1,τ) pairs considered.

To find the duration of the initial phase τ_1 maximizing the therapeutic window, the thresholds of rupture and mild coagulation were estimated. Temperature rise of 143ºC was defined as a threshold of vaporization and retinal rupture, corresponding to a 180ºC temperature at vaporization and 37ºC ambient temperature in

accordance with previous measurements[14]. In calculating the powers that brought peak temperature up to this threshold, the Z_{int} term was modified to include an 11 µm "hot-spot" of elevated absorption coefficient corresponding to pigmentation inhomogeneities. Mild coagulation thresholds were estimated as the power at each duration that brought the Arrhenius integral (Eqn. 1) up to corresponding Arrhenius value in the full finite-element model of retinal coagulation[14]. Initial phase durations (τ_1) of 3.3, 6.4, and 11 ms maximized the therapeutic window for pulse durations of 5, 10 and 20 ms, respectively, with pulses decaying down to 0.63, 0.71 and 0.76 of the peak amplitude along the optimized splines. An optimal pulse shape calculated for a 10 ms duration pulse is shown in Figure 1.

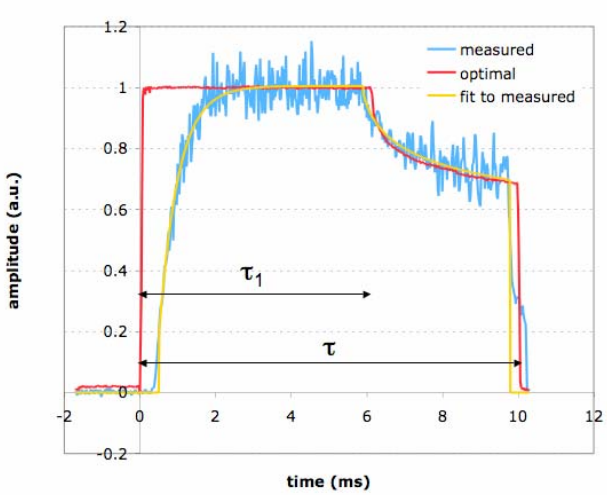

Fig. 1. Computed optimal (red), measured experimental (blue), and fit to experimental (yellow) pulse shapes for 10 ms duration.

2.2 Finite-element computational model

For both the shaped pulse and shaped beam, a finite-element model of retinal heating and coagulation in rabbit[14] was used to estimate threshold power and safe therapeutic window. This model approximated the retina as a series of homogeneous absorbing layers and coupled an axi-symmetric heat conduction model with an Arrhenius damage model. As opposed to the simplified semi-analytical model used to optimize the pulse shape, this model incorporated retinal absorption and scattering, a stratified choroid (choriocapillaris, pigmented choroid, unpigmented deep choroid), experimentally measured in-eye beam shape and power transmission, and calculated the temperature and Arrhenius integral maps over the entire retinal thickness. This model was implemented using the COMSOL Multiphysics 3.5 computational package[15].

Several modifications to the original model[14] were incorporated in this study. In the shaped beam computations, ring-beam images from *in vivo* experiments (Sec. 2.3) were normalized to their surface integral and a fit function of the form:

$$I(r) = A_0\left(\exp\left(-\left(\frac{r-r_0}{w_0}\right)^2\right)+\exp\left(-\left(\frac{r+r_0}{w_0}\right)^2\right)\right)+A_1\left(1+erf\left(\frac{r_1-r}{w_1}\right)\right) \quad (4)$$

was selected in order to account for both the TEM_{00} (fundamental) and TEM_{01}* ("doughnut") radial modes in the experimental beam[16], where A_0, A_1, r_0, r_1, w_0 and w_1 are fit parameters. A numerical optimization for the 6 parameters was performed in MATLAB 7.4 for each beam image, and average parameter values were used to give a functional description of the irradiance distribution on the retina. A sample ring-beam profile and the average fit are shown in Figure 2 (inset). The original error-function fit to the *in vivo* beam shape measured in the original model[14] was used for the flat-top beam and shaped pulse computations. Additionally, a 9 µm annular strip at the irradiance maximum of the ring-shaped beam served the function of the central 22 µm diameter hotspot in the original model. This central hotspot was unrealistic for modeling RPE pigmentation-based overheating for a ring-shaped beam in an axi-symmetric computational domain.

An approximation to the measured experimental pulse shape was used to describe the temporal variation of the laser source. This included both an exponential rise-time of 600 µs and a fit to the measured decay (Figure 1). Additionally, a threshold for mild coagulation was computed, assuming that it occurred when an Arrhenius value of 1 was reached at a radius of 50 µm and depth of 5 µm, corresponding to destruction of photoreceptor outer segments at a radius large enough to be visible ophthalmoscopically. As in the original model, rupture was computed as the power to bring peak temperature to 180ºC with the inclusion of either a central 11 µm hotspot or annular 9 µm hotspot of elevated absorption coefficient.

2.3 Optoelectronic setup

A modified slit lamp (Zeiss, SL 130) was used to support the delivery of the ring-shaped laser beam and provide a view of the fundus (Figure 2). The optical radiation from a diode-pumped continuous-wave frequency-doubled (532 nm wavelength) Nd:YLF laser (MP532-3W, Monocrom) was coupled into a 200 µm core diameter multimode optical fiber (FG200LCC, Thorlabs, Inc., Newton, NJ). A ring-shaped illumination pattern was achieved by coupling the beam into the fiber tip at an angle (~5º) with respect to normal incidence. This particular coupling method results in excitation of a combination of the TEM_{00} and TEM_{01}* modes supported by the fiber. A plane near the exit surface of the fiber was imaged through an adapter attached to the slit lamp (LaserLink, Lumenis, Santa Clara, CA) onto the retina. At the aerial image plane of the slitlamp microscope, the full-width-half-max (FWHM) spot size measured 260 µm, with the laser irradiance transition from 10% to 90% occurring over 35 µm on the external edge of the ring. Variation of the beam irradiance due to speckling along a circular contour coinciding with the irradiance maximum did not exceed 20%. A central amplitude modulation of 75% was used. (Figure 2 inset). The aerial beam shape was imaged before every experiment to ensure that the same combination of the fiber modes was achieved.

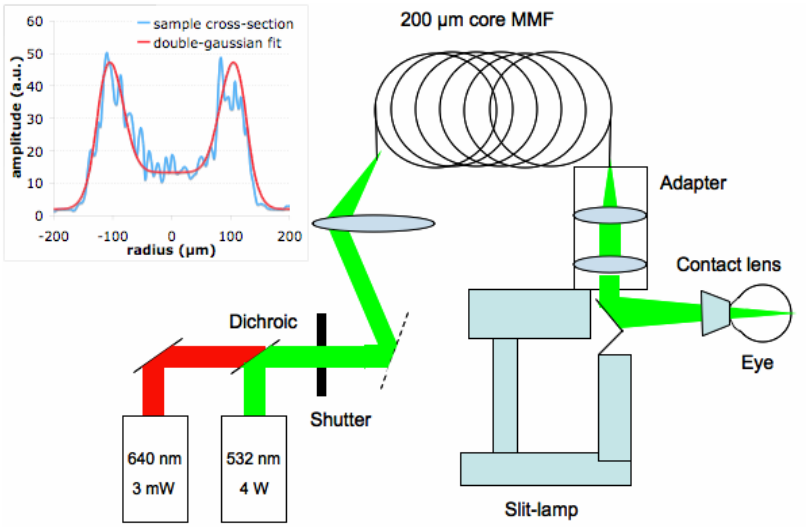

Fig. 2. Schematic for ring-beam photocoagulation setup. Ring-mode excitation is achieved through coupling into the multimode fiber (MMF) at an angle. A low-power 640 nm laser is coupled into the same mode for use as an aiming beam. A conventional slit lamp and fiber coupler serve as the delivery system. Inset: Sample aerial beam cross-section (blue) from experiments, with average functional fit (red) from Eqn. 4 used in computational modeling.

A graphical user interface (LabView, National Instruments Corp., Austin, TX) for the laser power supply (DS11, OSTech GmbH, Berlin) allowed for adjustment of duration and power, and a foot pedal activated the laser. A mechanical shutter was used to cut off the first 15 ms of the laser output to limit initial transient oscillations. This system was used to produce square pulses of 2 – 100 ms in duration, with intensity variations during the pulse of less than 10%. For comparison with the ring-shaped beam, a PASCAL photocoagulator (Optimedica, Santa Clara, CA) was used to produce a flat-top beam (200 µm aerial spot-size) and square pulses with durations in the range of 2 – 100 ms.

To achieve shaped pulses, a trigger signal from the PASCAL photocoagulator was conditioned with a digital delay generator (DG535, Stanford Research Systems, Sunnyvale, CA) and used to gate the output of an arbitrary waveform generator (33120A, Agilent, Santa Clara, CA). A graphical user interface (LabView, National Instruments, Austin, TX) allowed for the pulse shape and amplitude from the waveform generator to be controlled. This interface was programmed with the optimal pulse shapes computed in the semi-analytic model. The shaped pulse was used as an input to the PASCAL laser driver, which modulated the power of the laser pulse according to the input waveform, as exemplified in Figure 1. Rise time for the pulse was less than 600 μs and intensity variations during the initial phase of constant power were less than 10%.

2.4 *In vivo* threshold measurements

Fourteen Dutch Belted rabbits (weight, 1.5-2.5 kg) were used in accordance with the Association for Research in Vision and Ophthalmology Resolution on the Use of Animals in Ophthalmic and Vision Research with approval from the Stanford University Animal Institutional Review Board. Ketamine hydrochloride (35 mg/Kg), xylazine (5 mg/Kg) and glycopyrrolate (0.01 mg/Kg) were used for anesthesia. Pupil dilation was achieved by 1 drop each of 1% tropicamide and 2.5% phenylephrine hydrochloride, and topical tetracaine hydrochloride 0.5% was used for local anesthesia. Both eyes of each rabbit were treated with ring-beam and flat-top exposures to allow for direct comparison of the relative safety of each treatment on an eye-to-eye basis. Exposures of 2, 5 and 10 ms were placed in one eye of each animal and 20, 50 and 100 ms exposures were placed in the fellow eye. Eleven of the rabbits were also treated with shaped-pulse exposures in each eye. Pulses of 5 and 10 ms were placed in one eye of each animal and 20 ms exposures were placed in the fellow eye.

The threshold powers of mild coagulation and rupture at each pulse duration were measured for the two beam shapes. These thresholds were also recorded for square and modulated pulses with the flat-top beam shape. Between 12 and 36 separate lesions were administered per eye for each beam shape, pulse shape, and pulse duration. Power was titrated to produce lesions with clinical grades ranging from invisible to rupture. A standard retinal laser contact lens (OMSRA-S; Ocular Instruments, Bellevue, WA) was placed onto the mydriatic eye using hydroxypropyl methylcellulose as a contact gel. Taking into account the combined magnifications of the contact lens and rabbit eye of 0.66[17] the aerial images of 260 μm for the ring-beam and 200 μm for the flat-top beam corresponded to retinal spot sizes of 170 and 132 μm, respectively.

The clinical appearance of the laser lesions was graded by one observer within 3 seconds of delivering the laser pulse by means of the following scale: barely visible, mild, intense, and rupture. A barely visible lesion (often referred to as a minimally visible lesion, or MVL) was one that just crossed the limit of clinical detection and produced no whitening. A mild lesion was described as one that produced more significant blanching but no whitening. An intense lesion had an area of central whitening, with or without a ring of translucent edema. A rupture was assumed when a vapor bubble or discontinuity in retinal architecture was visualized with or without bleeding. Threshold powers for mild coagulation and rupture were calculated by Probit analysis in MATLAB 7.4[18]. The results were analyzed in terms of mean improvement in safe therapeutic window over the flat-top beam (square pulse) results.

3. RESULTS

Mild coagulation and rupture threshold powers are shown in Figure 3. Average Probit slope (ED84/ED50) for the threshold measurements was 1.09 for the ring-shaped beam, 1.15 for the modulated pulse, and 1.07 for the square pulse (flat-top beam). The mean safe therapeutic window appeared to increase logarithmically with pulse duration for both beam shapes and pulse shapes (Figure 4a, 4b), similarly to previous measurements[10]. For the ring beam, an improvement in therapeutic window was observed at all durations between 5 ms and 100 ms, while an improvement was seen at 5 ms and 10 ms with the shaped pulse.

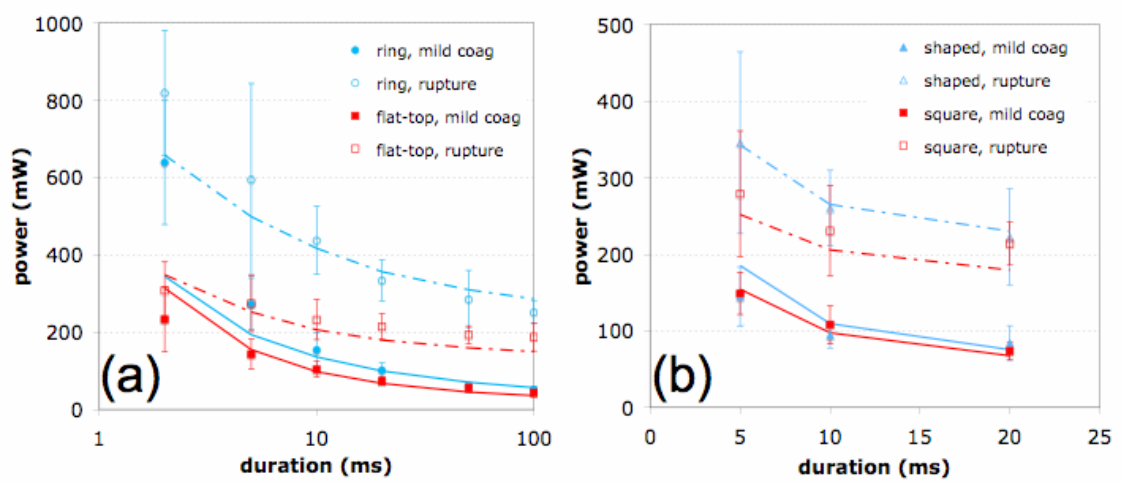

Fig. 3. (a) Mild coagulation and rupture thresholds for ring-beam (blue) and flat-top beam (red) as a function of pulse duration. Error bars indicate standard deviation in threshold measurements over 14 rabbits. Lines indicate model predictions. (b) Mild coagulation and rupture thresholds (peak power) for shaped pulse (blue) and square pulse (red) as a function of pulse duration. Error bars indicate standard deviation in threshold measurements over 11 rabbits.

The therapeutic window (TW) is expected to have a ratio statistical distribution, with the underlying threshold laser powers following correlated normal distributions. This ratio distribution deviates significantly from normal, making non-parametric hypothesis testing preferable[19]. Independently for the ring beam and shaped pulse thresholds, a paired permutation test was performed in MATLAB 7.4 against the flat-top, square pulse data for the null hypothesis that the measured therapeutic windows came from the same distribution[20,21]. For the ring beam, the increase in therapeutic window was found to be statistically significant ($p < 0.05$) for 10, 20 and 50 ms durations. The mean TW increase for 10 ms was +0.73 (95% CI: [0.27, 1.17]) while the increases for 20 ms and 50 ms were +0.42 [0.06, 0.77] and +1.27 [0.30, 2.22], respectively. These corresponded to percent-increases of 32.6% 14.3% and 36.3% over flat-top beam TW for 10, 20 and 50 ms durations, respectively. A small (<13%), statistically insignificant mean increase in TW was measured for 5 and 100 ms pulse durations, while a small decrease was observed for 2 ms. These results are summarized in Figure 4c. For modulated pulse, the increase in therapeutic window was found to be statistically significant ($p < 0.003$) for 5 and 10 ms, while the observed decrease at 20 ms was not ($p = 0.28$). The mean TW increase for 5 ms was +0.51 (95% CI: [0.31, 0.72]) while the increase for 10 ms was +0.61 [0.35, 0.88]. A small (7.5%) decrease in TW was measured for 20 ms pulse duration. These results are summarized in Figure 4d.

Estimated coagulation and rupture thresholds from the computational model are shown by lines in Figure 3 and modeled safe therapeutic window is shown in Figures 4a and 4b for both beam shapes and pulse types. Thresholds from the model were found to deviate less than 14% on average from the measured values (symbols). The therapeutic window deviated significantly at 5 and 10 ms for the modulated pulse due to overestimation of the coagulation threshold. At these durations, an improvement of approximately 14% was predicted, rather than the 28% increase actually observed.

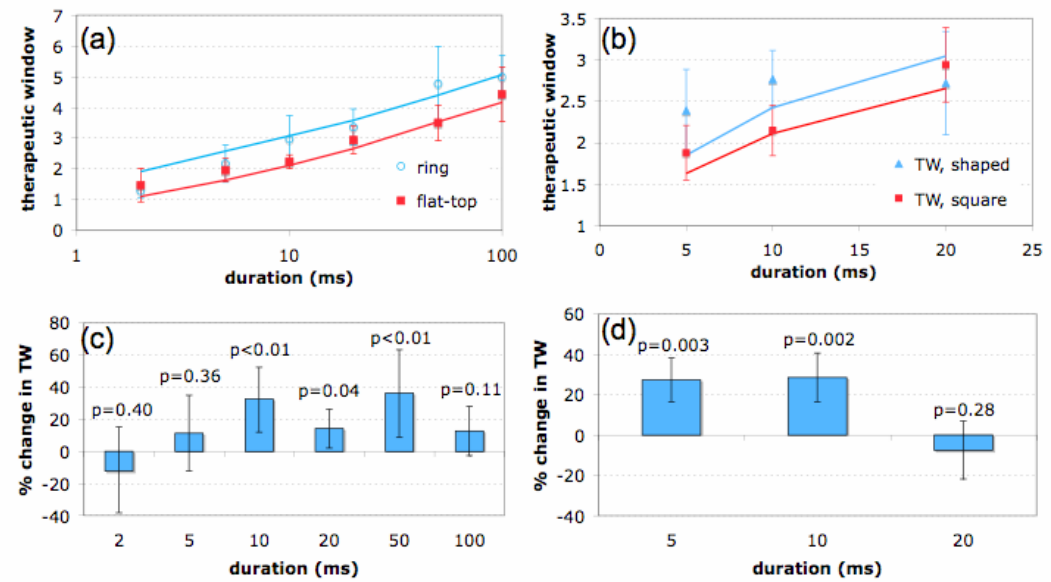

Fig. 4. (a) Safe therapeutic window (TW), the ratio of rupture and mild coagulation thresholds, as a function of duration for ring beam (blue) and flat-top beam (red). Predicted TW from the computational model is indicated by solid lines. (b) Safe therapeutic window for modulated pulse (blue) and square pulse (red) along with computational model predictions. (c) Percent difference in safe TW between ring beam and flat-top beam with 95% confidence intervals. Permutation test p-values are indicated. (d) Percent difference in safe TW between modulated and square pulses.

4. DISCUSSION

The goal of this work was to evaluate potential improvements in safety during short-pulse photocoagulation with a ring-shaped beam and modulated laser pulses. The measured improvement in safe therapeutic window for both treatments indicates that this is possible. The ring beam used in this study had larger than optimal modulation depth due to experimental convenience of maximizing power coupling into the ring mode. Further improvement may be expected with a modulation depth reduced to approximately 50%. Additionally, although the experimental pulse shapes used were a close approximation to the computed optimal shapes, there are additional aspects of the optimization and experimental implementation that should be considered.

As in most *in vivo* measurements, several factors limited the accuracy in determination of threshold powers for coagulation and rupture. Measurement of the coagulation threshold is inherently a subjective process, and the distinction between a minimally visible lesion and mild coagulation is particularly sensitive to the judgment of the clinician. While the MVL threshold is more objective, as it depends solely on visibility rather lesion character, the mild coagulation threshold is more clinically relevant and more familiar as a photocoagulation endpoint to the clinician. We attempted to control for subjectivity by using the same lesion judgment criteria for both beam types and both pulse types, pairing threshold measurements by placing different types of lesions in each eye, and using a single observer for all experiments.

Another aspect affecting threshold measurements is focusing errors during the treatment. Although the use of a parafocal photocoagulation system and contact lens provides for convenient focusing[22], errors in focusing are inevitable during photocoagulation. Focusing will vary slightly from exposure to exposure, with the degree of defocusing depending upon the skill and fatigue of the surgeon and the animal's level of anesthesia. The ring-shaped beam will defocus in a different manner than a flat-top beam: for positive or negative focal errors, the ring beam central modulation decreases while the flat-top beam become more Gaussian in shape. Although broadening of the beam will likely result in increased TW relative to the in-focus case for both beams, the lack of central overheating for with the ring beam may make it less sensitive to defocusing.

Other limitations on threshold measurements also relate to variations in laser energy deposition. RPE pigmentation varies by about a factor of two across the human population[23]. There is also variation between species as well as across the fundus of a given eye, with variations as high as a factor of three from macula to periphery[24,25]. Paired therapeutic window measurements and averaging over multiple test eyes helps control for this variation. Laser pulse energy varies as a function of pulse duration and shot-to-shot due to intensity fluctuations of 10% and mechanical shutter timing jitter of ~300 μs. Direct measurement of laser pulse energy variation before each experiment allowed for this uncertainty to be included in the Probit analysis.

The simplified semi-analytical model used for optimizing the pulse shape did not include several aspects that affect the temperature distribution in the retina, namely neuro-retinal absorption and scattering, a highly absorbing pigmented choroidal layer and a tapered flat-top irradiance distribution. The FWHM diameter of ~100μm for the irradiance distribution used in the full finite-element model[14] implies a heat diffusion time $\tau_d = L^2/4k = 16.6$ ms (where k is the thermal diffusivity of liquid water). This indicates that the temperature reaches a steady-state by the end of the 20 ms pulse, and thus the potential for improvement with shaping of the pulses of 20 ms or longer should be minor. This was indeed confirmed by experiment – no significant improvement was observed for 20 ms pulses.

A limitation in precision of the semi-analytical model used to optimize the pulse shape was the simplified criterion for estimating mild coagulation. This criterion was based solely on the central Arrhenius value and may have been overly conservative. The threshold Arrhenius values used for this criterion were estimated in the full finite-element model and corresponded to a smaller, tapered flat-top irradiance distribution. With this beam shape, a higher peak Arrhenius value might be expected than with the non-tapered flat-top distribution assumed in the semi-analytical model. This would lead to an overestimation of the required peak temperature and initial phase length τ_1, which may have negated any benefit from pulse shaping, particularly at the 20 ms pulse duration.

Practical clinical implementation of modulated-pulse and ring-beam photocoagulation will require few modifications to the systems used in this study. In diode-pumped solid state laser systems (such as the frequency-doubled Nd:YAG laser used in the photocoagulator), adjustment of the laser power during the pulse requires only analog modulation of the laser pump current. If the laser is computer-controlled, additional software could adjust the pulse shape for various pulse durations. A ring beam can be produced by coupling the laser into the fiber at an angle, and adjusting the coupling angle allows for variation of the mode structure and associated modulation depth of the beam. Alternative methods for shaping the beam should also be explored, such as masking the fiber tip or the using spatial light modulators.

Apart from ophthalmoscopic lesion appearance, ring-beam and modulated-pulse lesion character was not explored in this study. Histological analysis of the lesions will be necessary in order to show photoreceptor destruction comparable to the conventional photocoagulation. In ring coagulation, the presence of a central region of under-coagulated retina may also affect lesion healing, as viable central photoreceptors may lead to more rapid photoreceptor migration throughout the lesion.

Important clinical implications will arise if the measured improvement in safe therapeutic window can be duplicated in human subjects. Pigmentation varies across the fundus, which requires a safe therapeutic window on the order of three for any clinically applicable treatment[14]. Photocoagulation with a ring beam or shaped pulse allows for a therapeutic window of nearly three to be achieved at 10 ms rather than 20 ms required with a conventional flat-top beam and square pulse. The therapeutic window of 2.4 at 5 ms for shaped pulse is also promising. With further refinement of the pulse shape, this duration may also be made safe. Such reduction in pulse duration would allow for up to a four-fold increase in the number of lesions placed during eye fixation time with patterned scanning, reducing the overall treatment time by 75%. It might also further reduce heat diffusion into the neural retina and decrease perceived pain due to limited heat diffusion into the choroid, potentially resulting in a marked improvement over current photocoagulation standards.

ACKNOWLEDGEMENTS

The authors thank Drs. Loh-Shan Leung and Theodore Leng for help with animal handling, Georg Schuele for assistance with PASCAL, Alex Chang for laboratory support and software expertise, Nicholas Henderson for discussions on optimization methodology, and Ryan Tibshirani for guidance with the statistical analysis. Funding was provided by the US Air Force Office of Scientific Research (MFEL Program) and the Stanford Photonics Research Center. Disclosure: DP holds a Stanford University patent on patterned scanning laser photocoagulation licensed to OptiMedica Corporation with an associated equity and royalty interest and serves as a consultant for OptiMedica Corporation. CS and DP are party to a Stanford University patent application for shaped beam and modulated pulse photocoagulation.

REFERENCES

[1] Little, H.L., Zweng, H.C. and Peabody, R.R. “Argon laser slit-lamp retinal photocoagulation,” Trans Am Acad Ophthalmol Otolaryngol 74, 85-97 (1970).
[2] “Treatment techniques and clinical guidelines for photocoagulation of diabetic macular edema. Early Treatment Diabetic Retinopathy Study Report Number 2,” Early Treatment Diabetic Retinopathy Study Research Group. Ophthalmology 94, 761-74 (1987).
[3] “The influence of treatment extent on the visual acuity of eyes treated with Krypton laser for juxtafoveal choroidal neovascularization,” Macular Photocoagulation Study Group. Arch Ophthalmol 113, 190-4 (1995).
[4] Kapany, N.S., et al. “Retinal Photocoagulation by Lasers,” Nature 199, 146-9 (1963).
[5] Mainster, M.A. “Decreasing retinal photocoagulation damage: principles and techniques,” Seminars in Ophthalmology 14, 200-9 (1999).
[6] Blumenkranz, M.S., Yellachich, D., Andersen, D.E., Wiltberger, M.W., Mordaunt, D., Marcellino, G.R. and Palanker, D. “Semiautomated patterned scanning laser for retinal photocoagulation,” Retina 26, 370-6 (2006).
[7] Al-Hussainy, S., Dodson, P.M. and Gibson, J.M. “Pain response and follow-up of patients undergoing panretinal laser photocoagulation with reduced exposure times,” Eye 22, 96-9 (2008).
[8] Roider, J., Hillenkamp, F., Flotte, T. and Birngruber, R. “Microphotocoagulation - Selective Effects of Repetitive Short Laser-Pulses,” Proceedings of the National Academy of Sciences of the United States of America 90, 8643-8647 (1993).
[9] Obana, A. “The therapeutic range of chorioretinal photocoagulation with diode and argon lasers: an experimental comparison,” Lasers and Light in Ophthalmology 4, 147-156 (1992).
[10] Jain, A., Blumenkranz, M.S., Paulus, Y., Wiltberger, M.W., Andersen, D.E., Huie, P. and Palanker, D. “Effect of pulse duration on size and character of the lesion in retinal photocoagulation,” Arch Ophthalmol 126, 78-85 (2008).
[11] Niemz, M. [Laser-Tissue Interactions: Fundamentals and Applications], Springer, Berlin (2002).
[12] Simanovskii, D.M., Mackanos, M.A., Irani, A.R., O'Connell-Rodwell, C.E., Contag, C.H., Schwettman, H.A. and Palanker, D.V. “Cellular tolerance to pulsed hyperthermia,” Phys Rev E Stat Nonlin Soft Matter Phys 74, 011915 (2006).
[13] Birngruber, R., Hillenkamp, F. and Gabel, V.P. “Theoretical Investigations of Laser Thermal Retinal Injury,” Health Physics 48, 781-796 (1985).
[14] Sramek, C., Paulus, Y., Nomoto, H., Huie, P., Brown, J. and Palanker, D. “Dynamics of retinal photocoagulation and rupture,” Journal of Biomedical Optics 14, 034007 (2009).
[15] COMSOL Multiphysics 3.5. COMSOL Inc. (http://www.comsol.com/) (2009).
[16] Yin, J., Gao, W. and Zhu, Y. “Generation of dark hollow beams and their applications,” In: Progress in Optics (Wolf, E., ed.), pp. 119-204, Elsevier Science B. V., Amsterdam (2003).
[17] Birngruber, R. “Choroidal circulation and heat convection at the fundus of the eye: implications for laser coagulation and the stabilization of retinal temperature,” In: Laser Applications to Medicine and Biology (Wolbarsht, M.L., ed.), pp. 277–361, Plenum Press, London (1991).
[18] Finney, D. [Probit analysis], University Press, London (1971).
[19] Hinkley, D. “On the ratio of two correlated normal random variables,” Biometrica 56, 635-639 (1969).
[20] Lehmann, E. [Testing statistical hypotheses], Springer, New York (2005).

[21] Good, P. [Permutation tests: a practical guide to resampling methods for testing hypotheses], Springer-Verlag, New York (1994).
[22] Frankhauser, F. “Lasers, optical systems and safety in ophthalmology: a review,” Graefe's Archive for Clinical and Experimental Ophthalmology 234, 473-487 (1996).
[23] Weiter, J., Delori, F., Wing, G. and Fitch, K. “Retinal pigment epithelial lipofuscin and melanin and choroidal melanin in human eyes,” Invest. Ophthalmol. Vis. Sci. 27, 145-152 (1986).
[24] Lappin, P.W. and Coogan, P.S. “Relative sensitivity of various areas of the retina to laser radiation,” Archives of Ophthalmology 84, 350-4 (1970).
[25] Gabel, V.P., Birngruber R, Hillenkamp F. “Visible and near infrared light absorption in pigment epithelium and choroids,” Congress Series: XXIII Concilium Ophthalmologicum 450, 658-662 (1978).